scientific reports

Check for updates

OPEN

JS-K induces ferroptosis in renal carcinoma cells by regulating the c-Myc-GSTP1 Axis

Yuwan Zhao[1,2], LuGang Zhu[1,2], Xinghua Lin[1], Bin Li[1], Bailiang Miu[1], Jingping Qiu[1], Sheng Gao[1] & Jianjun Liu[1]✉

JS-K is a precursor drug of nitric oxide (NO) and inhibits tumor growth through various mechanisms. Ferroptosis, a form of cell death closely related to lipid peroxidation, is increasingly being recognized for its role in cancer biology. However, the relevance of ferroptosis in the anti-tumor effects of JS-K is yet to be defined. The cytotoxic effects of erastin and JS-K were evaluated in various renal cell carcinoma (RCC) cell lines and normal human renal epithelial cells. Cell viability and the intracellular levels of ferrous ions, glutathione (GSH), lipid peroxides, and malondialdehyde (MDA) were measured using standard in vitro assays. The expression levels of specific proteins were analyzed by western blotting. Subcutaneous xenografts of RCC were established in a nude mouse model, and the anti-tumor effects of JS-K were assessed by histological and immunohistochemical methods. Erastin selectively inhibited the growth of RCC cells without affecting normal renal cells. In addition, JS-K induced ferroptosis in RCC cells by reducing cellular GSH levels, increasing lipid peroxidation, and elevating ferrous ion levels, and the effects of JS-K were neutralized by N-acetylcysteine (NAC). At the molecular level, JS-K downregulated GSTP1 by blocking the transcription factor c-Myc. Finally, JS-K inhibited tumor growth in a mouse model by inducing ferroptosis. JS-K induces ferroptosis in RCC cells by depleting glutathione through the inhibition of the c-Myc-GSTP1 axis.

Keywords Renal cell carcinoma, JS-K, c-Myc, GSTP1, Ferroptosis

Abbreviations

RCC	Renal cell carcinoma
ccRCC	Clear cell renal cell carcinoma
GST	Glutathione S-transferase
NO	Nitric Oxide
SLC7A11	Solute carrier family 7 member 11
GPX4	Glutathione Peroxidase 4
GSH	Glutathione
GSTP1	Glutathione S-transferase pi-1

Renal cell carcinoma (RCC) is the most prevalent type of kidney cancer. Advanced RCC is particularly challenging to treat due to the rapid development of drug resistance. Studies show that compared to other tumors[1,2], RCC is more sensitive to the ferroptosis inducer erastin[3]. However, it remains to be ascertained whether ferroptosis could serve as a new therapeutic target for RCC.

JS-K is a nitric oxide (NO) prodrug that triggers spontaneous release of NO through the catalytic activity of glutathione S-transferase (GST) in the presence of glutathione (GSH)[4]. GSTs possesses three primary functions: catalyze the conjugation of oxidative stress and exogenous substances with reduced glutathione, bind to non-enzymatic substrates, and participate in protein-protein interactions[5,6]. Studies have established the anti-tumor effects of JS-K in various cancers, The cell types involved include leukemia cells, prostate cancer cells, bladder cancer cells, and renal cancer cells. Among these, The combination of JS-K and metformin induces DNA double-strand breaks in renal cancer cells, leading to cell death. However, the mechanism by which JS-K inhibits the proliferation of renal cancer cells on its own remains unclear[4–8].

Ferroptosis is a form of programmed cell death characterized by the massive accumulation of lipid peroxides and ferrous ions[9,10]. GSTP1, a member of the GST isoenzymes, protects cells from ferroptosis by catalyzing the

[1]Laboratory of Urology, Affiliated Hospital of Guangdong Medical University, 57 Renmin Street South, Zhanjiang 524001, Guangdong, China. [2]These authors contributed equally: Yuwan Zhao and LuGang Zhu. ✉email: jianjunliulab@163.com

conjugation of GSH with lipid peroxides, independent of the previously reported ferroptosis defense system[11]. Yang et al. showed that RCC cells are highly susceptible to ferroptosis[3]. There is evidence suggesting that JS-K can deplete glutathione, a crucial component of the antioxidant system, in leukemia cells. The VHL gene is frequently deleted in clear cell renal cell carcinoma (ccRCC). Miess et al. showed that deletion of the VHL gene inhibits β-oxidation and mitochondrial ATP synthesis, resulting in the accumulation of lipid peroxides due to reduced lipid metabolism. As a result, VHL-deficient ccRCC cells are sensitive to ferroptosis[12]. Therefore, ferroptosis induction through the depletion of intracellular glutathione can be explored as a potential therapeutic strategy for renal cancer. We had previously shown that JS-K down-regulates c-Myc in leukemia cells[5] and kidney cancer cells. Given that c-Myc regulates GSH metabolism and ferroptosis-related genes[12–16], the aim of this study was to explore the relationship between c-Myc and ferroptosis in RCC, and the therapeutic potential of JS-K.

Methods

Cell culture

The human RCC cell lines 786-O and A498, and the renal epithelial cell line HK-2 were obtained from the Chinese Academy of Sciences Cell Bank (CAS Cell Bank, Beijing, China). The RCC cells were cultured in Roswell Park Memorial Institute 1640 (RPMI-1640) medium supplemented with 10% fetal bovine serum (FBS, ZETA). The HK-2 cells were cultured in Dulbecco's Modified Eagle's medium (DMEM) supplemented with 10% FBS (ZETA). All cultures were maintained in a humidified incubator at 37℃ in an atmosphere containing 5% CO_2.

Cell viability assay

The cells were seeded in a 96-well plate at the density of 3000 cells/well and cultured overnight. Erastin (5 μM for 786-O cells, 2 μM for A498 cells) was added to the medium either alone or in combination with ferrostatin-1 (5 μM for 786-O cells, 2 μM for A498 cells), and the cells were incubated for 24 h. In another experiment, JS-K (4 μM, Santa Cruz) was added with or without NAC (200 μM), Z-VAD-FMK (30 μM), liproxstatin-1 (100 μM), CQ (50 μM), and necrostatin-1 (40 μM). At pre-determined time points, 10 μl CCK-8 solution (Dojindo) was added to each well, and the cells were incubated for 1 h. The absorbance at 450 nm was measured using a microplate reader, and cell viability was calculated based on the absorbance values.

Western blotting

The suitably treated cells were lysed using RIPA buffer supplemented with PMSF under ice-cold conditions. The protein samples were separated by sodium dodecyl sulfate-polyacrylamide gel electrophoresis (SDS-PAGE) and transferred onto a polyvinylidene fluoride (PVDF) membrane. After blocking with 5% skim milk, the membrane was incubated overnight with the primary antibody at 4 °C, followed by horseradish peroxidase-labeled secondary antibody (1:10,000) for 1 h at room temperature. The grayscale values of the protein bands were analyzed using Image J software, with GAPDH as the internal reference.

Lentivirus transduction

A lentiviral construct with c-Myc-specific siRNA (si-c-Myc) and the control empty vector were obtained from GenePharma Biotechnology Company (Suzhou, Jiangsu, China). The RCC cells were transfected with si-c-Myc and a non-targeting siRNA (si-NC) at a transfection ratio of 1:25. The stably transfected cells were selected with a suitable concentration of puromycin.

Lipid peroxidation analysis

The cells were seeded in a confocal dish at the density of 10^4 cells/well (786-O and HK-2 lines) or 1.5×10^4 cells/well (A498 cells). Following incubation with 4 μM JS-K, JS-K + 200 μM NAC, or 5 μM Erastin for 24 h, 10 μg/ml DAPI and BODIPY-581/591 C11 were added to each well. The cells were incubated for 30 min and serum-free medium was added. Live-cell imaging was performed using an OLYMPUS FV3000 laser scanning confocal microscope.

Fe^{2+} intensity assay

RCC cells were plated in a confocal dish at the density of 10^5 cells/well (786-O) or 1.5 × 10^5 cells/well (A498). Following incubation with 4 μM JS-K, JS-K + 200 μM NAC, or different doses of JS-K (0, 1, 2, 4 μM) for 24 h, 1 μM FerroOrange was added to each well. The cells were incubated for 30 min at 37 °C in a 5% CO_2 incubator, and live-cell imaging was performed using the OLYMPUS FV3000 laser scanning confocal microscope.

Measurement of intracellular MDA levels

Cells were cultured in a 10 cm cell culture dish till 70% confluent, and the medium was replaced with fresh drug-supplemented medium according to the experimental design. Following incubation for 24 h, the cells were lysed to extract the protein fraction. The concentration of protein in each sample was determined, and 200 μl MDA assay working solution was added to 100 μl of the lysates and mixed well. The samples were heated and centrifuged, and the supernatants were dispensed into a 96-well plate. The absorbance was measured at 532 nm using a microplate reader. The MDA content of the samples was determined using a standard curve, and expressed relative to the protein content by weight.

Measurement of intracellular GSH levels

Cells were cultured in a 10 cm cell culture dish till 70% confluent, and the medium was replaced with fresh drug-supplemented medium according to the experimental design. Following incubation for 24 h, the cells were harvested using trypsin. The samples were centrifuged, and the protein content of the supernatants was measured. Each sample was mixed with reagent one in a 1:1 ratio and centrifuged at 3500 rpm for 10 min. The

supernatants were collected, and 100 µl aliquots were dispensed into each well of a 96-well plate. Reagents two, three, and four were sequentially added according to the instructions, with a 5-min pause between the steps. The absorbance of each well was measured at 405 nm using a microplate reader. The measured values were then substituted into the formula to calculate the content of GSH.

Tumor xenografts

Female nude mice (BALB/c, nu/nu, 17–23 g, 4–5 weeks old) were obtained from SPF Biotechnology, Beijing, China, and housed under specific pathogen-free conditions on a 12 h/12 h light/dark cycle. The animal experiments were approved by the Ethics Committee for Animal Experimentation of Guangdong Medical University Affiliated Hospital, and were conducted in accordance with the Guidelines for the Care and Use of Laboratory Animals. All mice were subjected to an acclimatization period of at least 1 week before the experimental processes. Each mouse was subcutaneously injected with 10×10^6 control or c-Myc-knockout 786-O cells in 100 µl PBS. Once palpable masses had formed, the mice bearing the control and 786-$O^{c-Myc-/-}$ xenografts were randomly assigned to the placebo (0.9% saline solution) and JS-K (20 mg/kg) groups, and 100 µl of the respective formulations were injected through the tail vein three times per week for 6 weeks. The length (L) and width (W) of the tumors were measured every 7 days using calipers, and the tumor volume was calculated as: $V = \pi/6 \times L \times W^2$. The mice were euthanized on day 48 post-treatment by cervical dislocation after anesthetizing with 2% avertin. Tumor samples were harvested and processed for hematoxylin-eosin (HE) staining and immunohistochemistry (IHC).

Histological assessment and IHC

Tumor tissues sections were stained with HE for histological evaluation as per standard protocols. For IHC, the tissue sections were probed with anti-GSTP1 (Affinity Biosciences, DF7462, diluted 1:1000), anti-c-Myc (Fuzhou Maixin Biotech, RMA-0803, diluted 1:1000), and anti-KI67 (Proteintech, 27309-1-AP, diluted 1:2000) antibodies. Subsequently, the slides were incubated with goat anti-rabbit IgG H&L (HRP) secondary antibody (Abcam, ab6721, diluted 1:200).

Statistical analysis

GraphPad Prism version 9.3.1 (GraphPad Software, Inc., La Jolla, California, USA) was used for all statistical analyses. Quantitative data were initially tested for normality and homogeneity of variance. The normally distributed variables were described using mean ± standard deviation. Independent sample t-test was used to compare data between two groups, and analysis of variance (ANOVA) was utilized for comparisons among multiple groups. P value < 0.05 was considered statistically significant.

Results

Erastin induced ferroptosis in renal carcinoma cells

As shown in Fig. 1A, erastin decreased the viability of 786-O cells in a dose-dependent manner. Furthermore, the cytotoxicity of erastin was significantly higher in the 786-O cells compared to that in the normal renal epithelial cells (HK-2), especially at the concentration of 8 µM (Fig. 1A). BODIPY-C11 staining showed accumulation of lipid peroxidation products in the 786-O cells, but not in the HK-2 cells, following erastin treatment (Fig. 1B). The viability of erastin-treated 786-O (5 µM) and A498 (2 µM) cells also decreased in a time-dependent manner, while addition of ferrostatin-1 (2 µM for A498, 5 µM for 786-O) reversed the inhibitory effects of erastin (Fig. 1C).

A Viability of RCC (786-O) and normal human renal epithelial (HK-2) cells incubated with different concentrations of Erastin (0–8 µM) for 24 h. **B** Representative images showing oxidized lipid ROS (green color) and reduced lipid ROS (red color) in the suitably treated 786-O and HK-2 cells. Scale bars: 20 µm. **C** Viability rates of RCC cell lines incubated with Erastin (786-O 5 µM, A498 2 µM), Fer-1 (786-O 5 µM, A498 2 µM), or both, for 24, 48, or 72 h. The error bars represent the standard error of three replicates. $^{**}P < 0.01$, $^{****}P < 0.0001$.

JS-K May induce ferroptosis in RCC cells through depletion of glutione

Liproxstatin-1 partially inhibited JS-K-induced cell death, whereas inhibitors of caspase-mediated apoptosis (Z-VAD-FMK), necroptosis (necrostatin-1), or autophagy (chloroquine) had no impact (Fig. 2A), thus confirming that ferroptosis is the primary form of death induced by JS-K. On the other hand, the antioxidant N-acetylcysteine (NAC) rescued the RCC cells from the cytotoxic effects of JS-K (Fig. 2B), restored intracellular GSH levels (Fig. 2D), and reversed the increase in MDA (Fig. 2C), ferrous ions (Fig. 2E), and lipid peroxides (Fig. 2F) in the JS-K-treated cells. Taken together, these results suggest that JS-K induced ferroptosis in RCC cells by depleting GSH. JS-K decreased the expression levels of SLC7A11, GPX4, NCOA4, and FTH1, and increased that of TFR in the 786-O and A498 cell lines (Fig. 2G). Furthermore, JS-K reduced GSH levels (Fig. 2H), and increased the amount of MDA (Fig. 2I) and ferrous ions (Fig. 2J) in the RCC cell lines in a dose-dependent manner, which were indicative of ferroptosis.

JS-K induced ferroptosis in RCC cells by inhibiting the c-Myc/GSTP1 axis

Preliminary experiments had shown that JS-K decreased c-Myc protein expression in the 786-O and A498 cells (Fig. 3A), which suggested a role of c-Myc in JS-K-induced ferroptosis. To validate this hypothesis, we knocked down c-Myc in the RCC cells using a lentiviral si-RNA construct, and confirmed downregulation of the protein (Fig. 3B). JS-K treatment significantly reduced the viability of control and c-$Myc^{-/-}$ cells (Fig. 3C), and increased the intracellular MDA content (Fig. 3D). While NAC rescued the control cells from JS-K-induced ferroptosis, its protective effects were only partial in the c-$Myc^{-/-}$ cells (Fig. 3C, D). Furthermore, GSTP1 protein was downregulated in the JS-K-treated 786-O and A498 cells (Fig. 3E). Compared to the control cells, the c-$Myc^{-/-}$

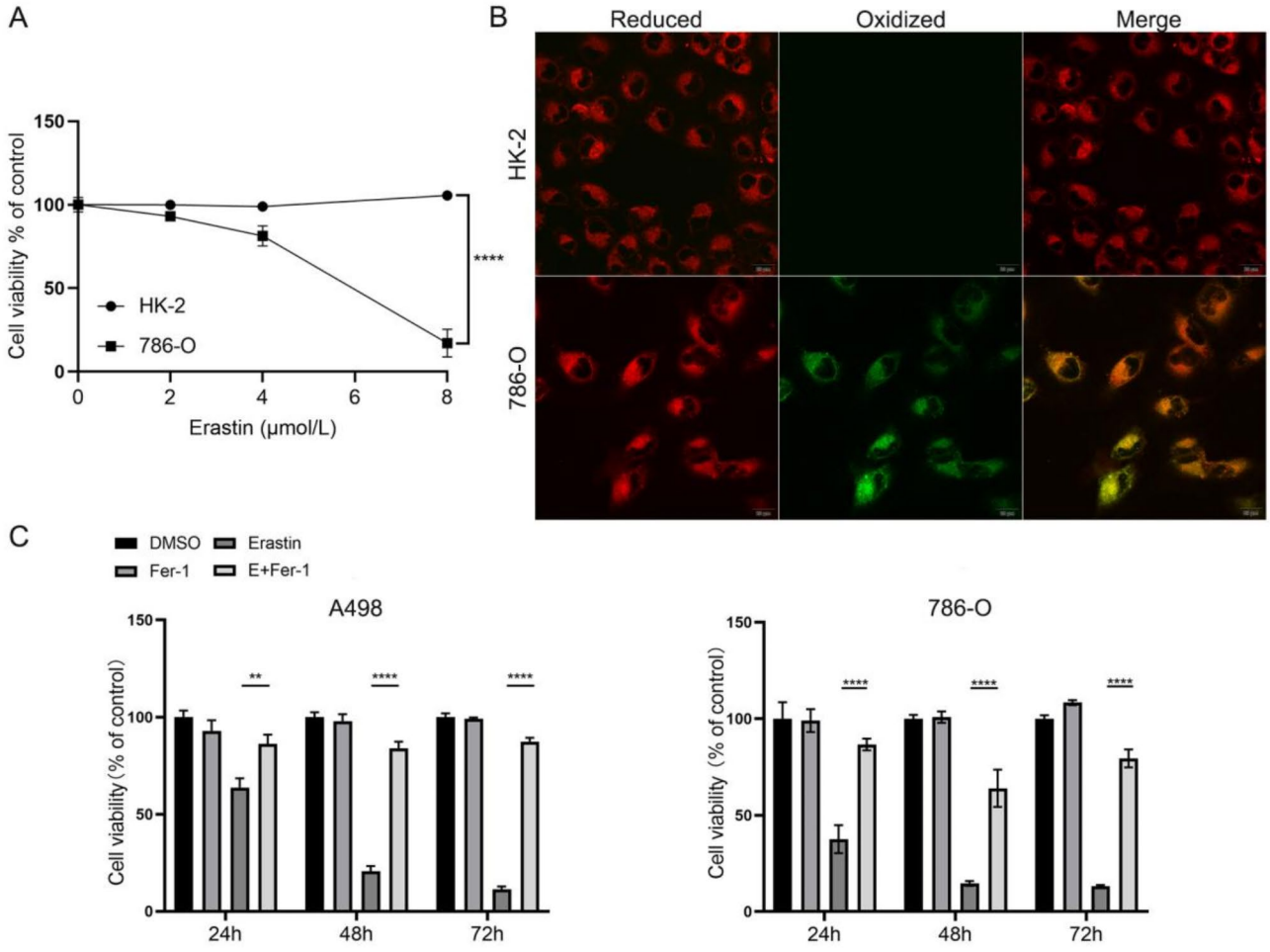

Fig. 1. Erastin induced ferroptosis in renal carcinoma cells.

cells also showed a significant decrease in GSTP1 protein (Fig. 3F). LiCl, which is known to upregulate c-Myc by activating the WNT pathway, rescued the inhibitory effect of JS-K on c-Myc and GSTP1 (Fig. 3G). Taken together, these results indicate that JS-K induces ferroptosis in RCC cells by targeting the c-Myc/GSTP1 pathway.

JS-K inhibited the growth of RCC xenografts in vivo

To determine the anti-tumor effects of JS-K or c-Myc depletion, we established subcutaneous xenografts of control and c-Myc$^{-/-}$ 786-O cells in athymic nude mice, and treated them with JS-K or placebo. The c-Myc$^{-/-}$ cells formed significantly smaller tumors compared to the control cells (Fig. 4A). Furthermore, JS-K treatment markedly reduced tumor volume and weight, and the effect was stronger against the c-Myc$^{-/-}$ tumors (Fig. 4B and C). Immunostaining of the tumor tissues showed lower in-situ expression of c-Myc and GSTP1 in the JS-K-treated and c-Myc$^{-/-}$ groups (Fig. 4D). Taken together, JS-K downregulated c-Myc and GSTP1 in vivo, which suggests that it might prevent RCC recurrence by inhibiting c-Myc.

Discussion

RCC is one of the most common malignancies of the urinary system. Surgery is the primary treatment for early-stage RCC, although nearly 40% of the patients develop metastatic disease (mRCC) after tumor resection. The poor response of patients with advanced RCC to the current therapeutic strategies has prompted researchers to seek new treatment options[17], such as the combination of radiotherapy and immunotherapy. Although RCC cells are not sensitive to radiotherapy, the concurrent use of radiation and immunotherapy drugs may exert a synergistic effect[18]. Additionally, novel targeted therapies are also being developed for RCC based on the molecular characteristics of the tumors. VHL, a key tumor suppressor gene, is frequently deleted in patients with clear cell RCC (ccRCC). Overexpression of VHL in ccRCC cells effectively inhibited ferroptosis by reducing the accumulation of lipid peroxides, whereas ccRCC cells with VHL gene deletion exhibited excessive accumulation of lipid peroxides[12]. Moreover, studies show that RCC cells are highly sensitive to ferroptosis inducers compared to other tumors cells[3], suggesting that ferroptosis could be a promising new target for RCC treatment.

JS-K inhibits tumor growth through various mechanisms. In leukemia cells for instance, the cytotoxic effects of JS-K are triggered by GSH depletion and the disruption of intracellular redox balance[5]. NAC reversed JS-K-induced apoptosis in bladder and prostate cancer cells, while the pro-oxidant glutathione disulfide (GSSG)

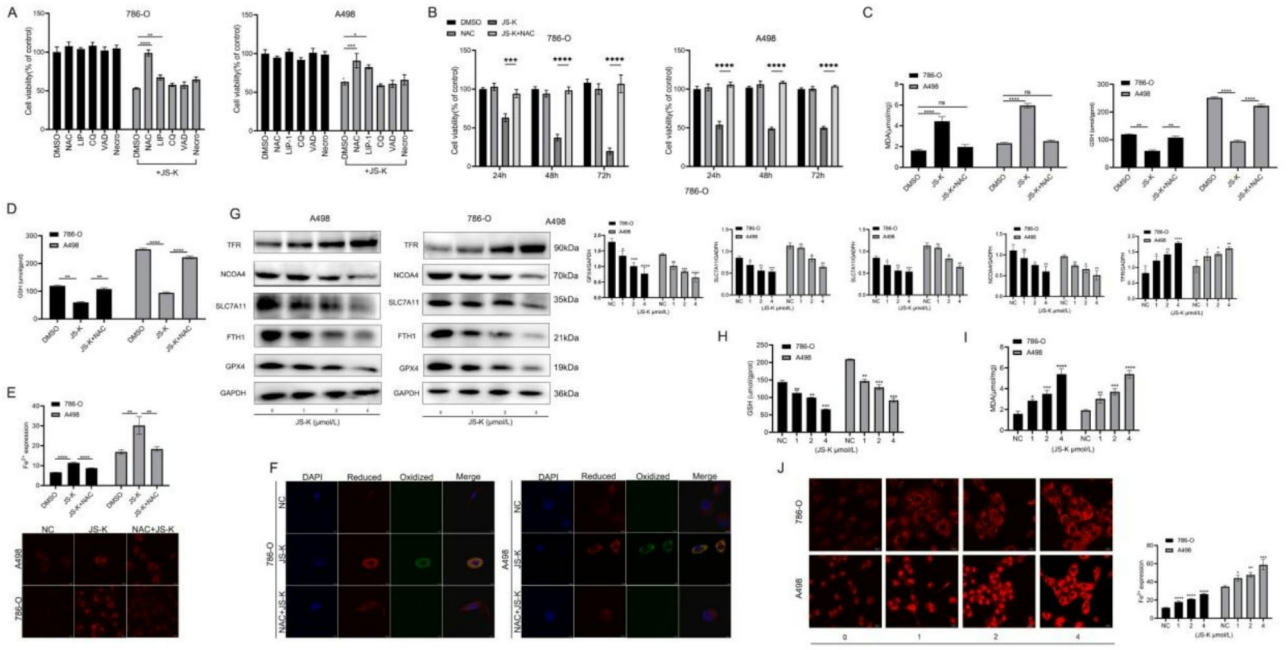

Fig. 2. JS-K may induce ferroptosis in RCC cells through depletion of glutione. **A** Viability rates of RCC cell lines (786-O and A498) incubated with JS-K (4 μmol/L), either alone or in combination with NAC (200 μmol/L), Z-VAD-FMK (30 μmol/L), Liproxstatin-1 (100 μmol/L), CQ (50 μmol/L), and Necrostatin-1 (40 μmol/L) for 24 h. **B** Viability rates of RCC cells incubated with JS-K (4 μmol/L) and NAC (200 μmol/L), and the combination of JS-K plus NAC for 24, 48, and 72 h. **C** MDA content in the RCC cells incubated with JS-K (4 μmol/L) and JS-K plus NAC (200 μmol/L) for 24 h. **D** GSH levels in RCC cells incubated with JS-K (4 μmol/L) and JS-K plus NAC (200 μmol/L) for 24 h. **E** Ferrous ion content in RCC cells incubated with JS-K (4 μmol/L) and JS-K plus NAC (200 μmol/L) for 24 h (scale bar: 20 μm). **F** Representative images showing lipid peroxidation in RCC cells incubated with JS-K (4 μmol/L) and JS-K plus NAC (200 μmol/L) for 24 h (scale bar: 10 μm). **G** Expression levels of SLC7A11, GPX4, NCOA4, FTH1, and TFR proteins in RCC cells incubated with different concentration of JS-K (0, 1, 2, 4 μmol/L) for 24 h. **H** GSH content in RCC cells incubated with different concentrations of JS-K (0, 1, 2, 4 μmol/L) for 24 h. **I** MDA content in RCC cells incubated with different concentrations of JS-K (0, 1, 2, 4 μmol/L) for 24 h. **J** Ferrous ion content in RCC cells incubated with different concentrations of JS-K (0, 1, 2, 4 μmol/L) for 24 h (scale bar: 20 μm).*$P<0.05$, **$P<0.01$, ***$P<0.001$,**** $P<0.0001$.

exacerbated the apoptotic effects of JS-K[6,7]. We had previously observed that JS-K inhibited the progression of RCC, although the exact mechanism was unclear. In this study, JS-K reduced the intracellular GSH content in RCC cells in a concentration-dependent manner, and the inhibitory effect of JS-K was neutralized by NAC. GSH is crucial for maintaining the intracellular redox homeostasis. Sodium molybdate also depletes GSH in cancer cells through a mechanism similar to that of JS-K[19]. Taken together, JS-K can induce ferroptosis in RCC cells by increasing the content of MDA and ferrous ions, and decreasing GSH content, eventually leading to tumor inhibition.

C-Myc regulates the transcription of γ-GCS gene under oxidative stress, and phosphorylation of c-Myc promotes GSH biosynthesis[20]. JS-K reduced the expression of c-Myc in myeloid leukemia cells at both the transcript and protein levels[21]. In addition, Maciag et al. had shown that JS-K significantly downregulated c-Myc protein expression in leukemia cells in a time-dependent manner[5]. Consistent with the above studies, JS-K decreased the expression of c-Myc in the RCC cells. Furthermore, exogenous NAC failed to rescue the c-Myc$^{-/-}$ cells from the inhibitory rate of JS-K, which could be attributed to a weaker reductive function of the GSH system in the absence of c-Myc.

GSTP1, a member of the GST isoenzyme family, promotes the combination of exogenous oxidants with GSH to maintain intracellular redox homeostasis[10,22,23]. In addition, GSTP1 and GSH are crucial components in the defense against ferroptosis and oxidative stress, and function independently of the initial ferroptosis defense mechanisms. In addition, studies indicate a link between the Myc family genes and GSTP1, and N-Myc has been identified as a direct regulator of GSTP1[24]. We found that GSTP1 was downregulated in the RCC cells following treatment with JS-K or c-Myc knockdown. The WNT pathway activator LiCl upregulated c-Myc in the JS-K-treated cells, and partially restored the expression of GSTP1. C-Myc regulates the expression of numerous genes at the transcriptional level, either directly or indirectly[25]. However, we did not explore the mechanism underlying the regulatory effect of c-Myc on GSTP1, or assess the impact of knocking down or overexpressing GSTP1.

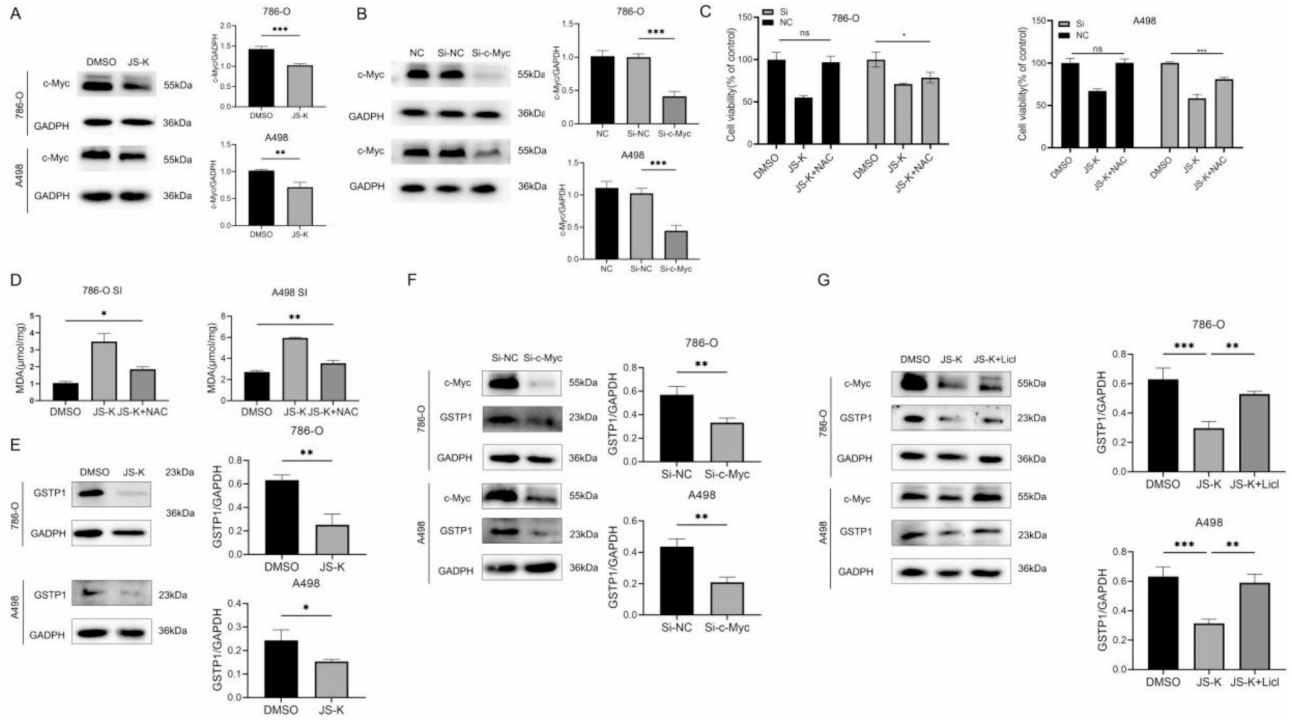

Fig. 3. JS-K induced ferroptosis in RCC cells by inhibiting the c-Myc/GSTP1 axis. **A** Changes in c-Myc protein levels in RCC cells (A498 and 786-O) following treatment with JS-K (4 μmol/L) for 24 h. **B** RCC cells with stable c-Myc knockdown (786-O$^{c-Myc-/-}$ and A498$^{c-Myc-/-}$) were constructed, and the knockdown efficiency was verified by western blotting. **C** Viability of control and c-Myc-/- RCC cells incubated with JS-K (4 μmol/L) and JS-K plus NAC (200 μmol/L) for 24 h. **D** MDA content in 786-O$^{c-Myc-/-}$ and A498$^{c-Myc-/-}$ cells incubated with JS-K (4 μmol/L) and JS-K plus NAC (200 μmol/L) for 24 h. **E** GSTP1 protein expression in RCC cells incubated with JS-K (4 μmol/L) for 24 h. **F** GSTP1 protein expression in control and c-Myc-/- RCC cells. **G** Expression levels of c-Myc and GSTP1 in RCC cells incubated with JS-K (4 μmol/L) and JS-K + LiCl (1 mmol/L) for 24 h. *$P < 0.05$, **$P < 0.01$, ***$P < 0.001$.

JS-K has been shown to inhibit the growth of various subcutaneous tumor xenografts in nude mice, including those for prostate cancer, multiple myeloma, and glioma[26–28]. We established subcutaneous tumors in nude mice using control and c-Myc$^{-/-}$ 786-O cells, and treated the tumor-bearing mice with JS-K or placebo. The depletion of c-Myc resulted in smaller tumors compared to that in the control group. In addition, JS-K significantly inhibited tumor growth in vivo, and the effect was stronger for the c-Myc$^{-/-}$ tumors. Furthermore, c-Myc, Ki67, and GSTP1 were relatively downregulated in the JS-K, c-Myc$^{-/-}$, and c-Myc$^{-/-}$ + JSK groups compared to the control group. In conclusion, JS-K can inhibit the growth of RCC by inducing ferroptosis and may hold significant therapeutic potential.

Conclusion

JS-K induces ferroptosis in RCC cells by binding to GSH and triggering ferroptosis through the regulation of the c-Myc-GSTP1 axis. Our findings provide new insights and potential therapeutic avenues for the treatment of RCC.

Limitations and future prospects

In this study, JS-K was found to inhibit the expression of c-Myc. However, we only utilized a c-Myc gene silencing model and did not employ an overexpression model. To further verify whether the inhibitory effect of JS-K on c-Myc expression is specific, additional exploration will be needed in future research. Moreover, the binding sites and regulatory mechanisms of the c-Myc/GSTP1 axis in renal cancer cells have not been fully elucidated. We plan to investigate these aspects in the future by exploring the molecular mechanisms of protein interactions.

In the in vivo experiment where JS-K inhibited the growth of renal cell carcinoma (RCC) xenografts, we focused primarily on the inhibitory effect of JS-K on the tumor xenografts themselves, as well as the detection of upstream regulatory factors c-Myc and GSTP1, since they are likely to play more important roles in the antitumor mechanisms of JS-K. However, the current results do not fully clarify whether JS-K induces ferroptosis in renal cancer cells. Future studies may consider supplementing the detection of ferroptosis-related indicators to further elucidate the mechanisms of action of JS-K.

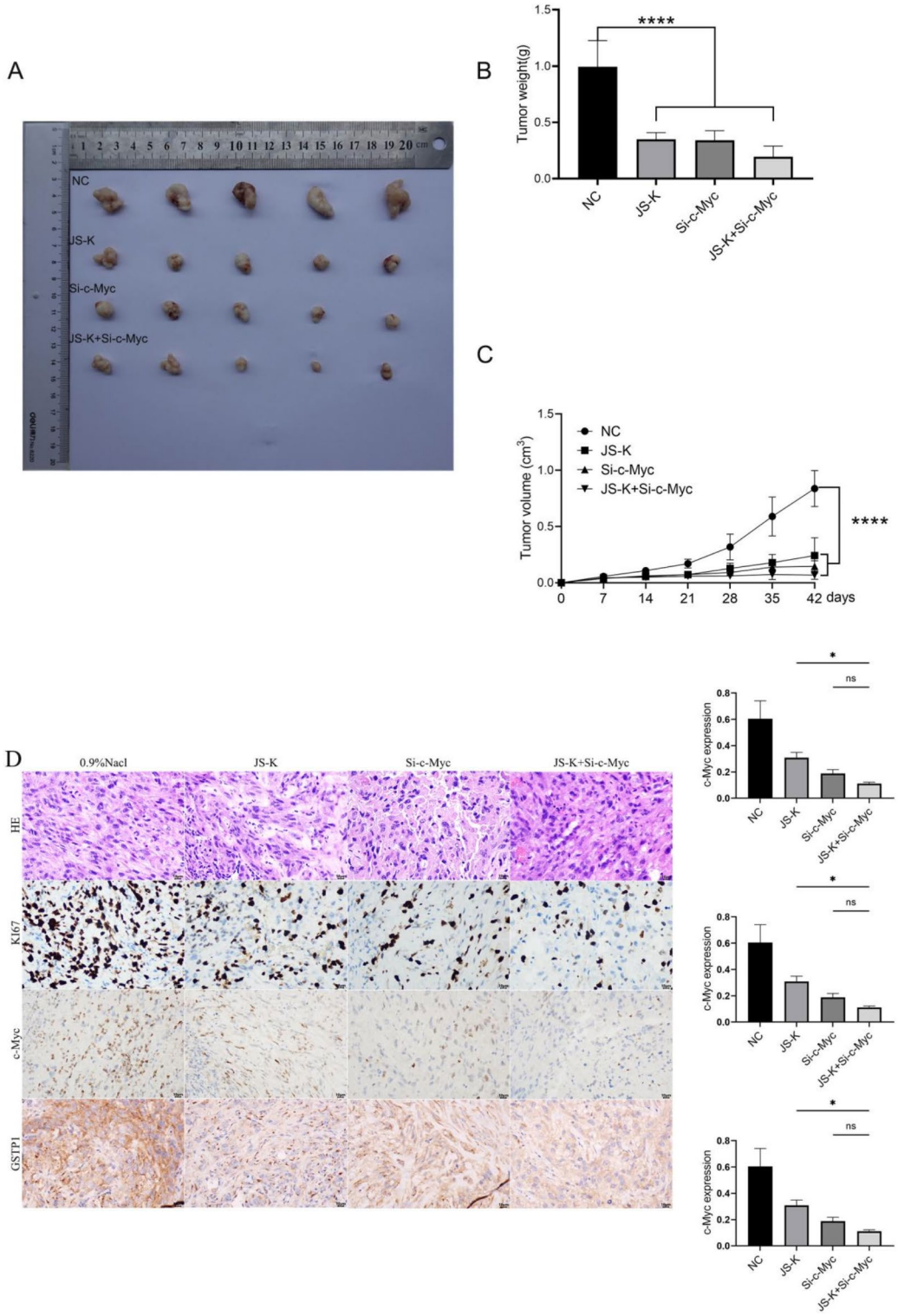

Fig. 4. JS-K inhibited the growth of RCC xenografts in vivo. **A** Representative images of tumor tissues excised from each group. **B** Mean tumor weight in each group. **C** Tumor volume in the indicated groups at different time points. **D** Representative immunohistochemistry (IHC) images showing expression of Ki67, c-Myc, and GSTP1 in each group (scale bar: 10 μm).*$P < 0.05$, **** $P < 0.0001$.

Data availability

All data generated during this study are included in this published article [and its supplementary information files], and the original data are available on request from the corresponding author.

Received: 5 December 2024; Accepted: 8 April 2025
Published online: 08 May 2025

References

1. Choueiri, T. K. et al. Nivolumab plus Cabozantinib versus Sunitinib for advanced renal-cell carcinoma. *N. Engl. J. Med.* **384** (9), 829–841 (2021).
2. Motzer, R. J. et al. Kidney cancer, version 3.2022, NCCN clinical practice guidelines in oncology. *J. Natl. Compr. Canc. Netw.* **20** (1), 71–90 (2022).
3. Yang, W. S. et al. Regulation of ferroptotic cancer cell death by GPX4. *Cell* **156** (1–2), 317–331 (2014).
4. Chakrapani, H. et al. Synthesis, mechanistic studies, and anti-proliferative activity of glutathione/glutathione Stransferase-activated nitric oxide prodrugs. *Bioorg. Med. Chem.* **16** (22), 9764–9771 (2008).
5. Maciag, A. E. et al. Nitric oxide-releasing prodrug triggers cancer cell death through deregulation of cellular redox balance. *Redox Biol.* **1** (1), 115–124 (2013).
6. Qiu, M. et al. A reactive oxygen species activation mechanism contributes to JS-K-induced apoptosis in human bladder cancer cells. *Sci. Rep.* **5**, 15104 (2015).
7. Qiu, M. et al. JS-K promotes apoptosis by inducing ROS production in human prostate cancer cells. *Oncol. Lett.* **13** (3), 1137–1142 (2017).
8. Zhao, Y. et al. Metformin in combination with JS-K inhibits growth of renal cell carcinoma cells via reactive oxygen species activation and inducing DNA breaks. *J. Cancer*. **11** (13), 3701–3712 (2020).
9. Dixon, S. J. et al. Ferroptosis: an iron-dependent form of nonapoptotic cell death. *Cell* **149** (5), 1060–1072 (2012).
10. Stockwell, B. R. et al. Ferroptosis: A regulated cell death nexus linking metabolism, redox biology, and disease. *Cell* **171** (2), 273–285 (2017).
11. Zhang, W. et al. SMURF2 predisposes cancer cell toward ferroptosis in GPX4-independent manners by promoting GSTP1 degradation. *Mol. Cell*. **83** (23), 4352–4369e8 (2023).
12. Miess, H. et al. The glutathione redox system is essential to prevent ferroptosis caused by impaired lipid metabolism in clear cell renal cell carcinoma. *Oncogene* **37** (40), 5435–5450 (2018).
13. Shroff, E. H. et al. MYC oncogene overexpression drives renal cell carcinoma in a mouse model through glutamine metabolism. *Proc. Natl. Acad. Sci. U.S.A.* **6** (3), 195–206 (2004).
14. Jin, Y., Qiu, J., Lu, X. & Li, G. C-MYC inhibited ferroptosis and promoted immune evasion in ovarian cancer cells through NCOA4 mediated ferritin autophagy. *Cells* **11** (24), 4127 (2022).
15. Lu, C. et al. Aberrant expression of KDM1A inhibits ferroptosis of lung cancer cells through up-regulating c-Myc. *Sci. Rep.* **12** (1), 19168 (2022).
16. Zhao, Y., Wang, Y., Miao, Z., Liu, Y. & Yang, Q. c-Myc protects hepatocellular carcinoma cell from ferroptosis induced by glutamine deprivation via upregulating GOT1 and Nrf2. *Mol. Biol. Rep.* **50** (8), 6627–6641 (2023).
17. Petros, F. G. et al. Oncologic outcomes of patients with positive surgical margin after partial nephrectomy: a 25-year single institution experience. *World J. Urol.* **36** (7), 1093–1101 (2018).
18. Kroeze, S. G. C. et al. Stereotactic radiotherapy combined with immunotherapy or targeted therapy for metastatic renal cell carcinoma. *BJU Int.* **127** (6), 703–711 (2021).
19. Mao, G. et al. Sodium molybdate inhibits the growth of ovarian cancer cells via inducing both ferroptosis and apoptosis. *Free Radic. Biol. Med.* **182**, 79–92 (2022).
20. Wahlstrom, T. & Henriksson, M. A. Impact of MYC in regulation of tumor cell metabolism. *Biochim. Et Biophys. Acta-Biomembranes*. **1849** (5), 563–569 (2015).
21. Liu, J. et al. Gene expression profiling for nitric oxide prodrug JS-K to kill HL-60 myeloid leukemia cells. *Genomics* **94** (1), 32–38 (2009).
22. Hayes, J. D., Flanagan, J. U. & Jowsey, I. R. Glutathione transferases. *Annu. Rev. Pharmacol. Toxicol.* **45**, 51–88 (2005).
23. Yin, Z., Ivanov, V. N., Habelhah, H., Tew, K. & Ronai, Z. Glutathione S-transferase P elicits protection against H2O2-induced cell death via coordinated regulation of stress kinases. *Cancer Res.* **60** (15), 4053–4057 (2000).
24. Fletcher Ji, Gherardi, S. et al. N-Myc regulates expression of the detoxifying enzyme glutathione transferase GSTP1, a marker of poor outcome in neuroblastoma. *Cancer Res.* **72** (4), 845–853 (2012).
25. Kress Tr, Sabò, A. & Amati, B. MYC: connecting selective transcriptional control to global RNA production. *Nat. Rev. Cancer*. **15** (10), 593–607 (2015).
26. Shami, P. J. et al. JS-K, a glutathione/glutathione S-transferase-activated nitric oxide donor of the diazeniumdiolate class with potent antineoplastic activity. *Mol. Cancer Ther.* **2** (4), 409–417 (2003).
27. Kiziltepe, T. et al. JS-K, A GST-activated nitric oxide generator, induces DNA double-strand breaks, activates DNA damage response pathways, and induces apoptosis in vitro and in vivo in human multiple myeloma cells. *Blood* **110** (2), 709–718 (2007).
28. Weidensteiner, C. et al. Effects of the nitric oxide donor JS-K on the blood-tumor barrier and on orthotopic U87 rat gliomas assessed by MRI. *Nitric Oxide*. **30**, 17–25 (2013).

Acknowledgements

We would like to thank MogoEdit (https://www.mogoedit.com) for its English editing during the preparation of this manuscript.

Author contributions

Y.Z. and L. Z. designed this study. Y. Z., L. Z., X. L. and B.M. performed the in vitro and in vivo experiment. Y. Z., and L. Z. analyzed the data. X. L., B. M., J. Q. and S. G. discussed this project. Y. Z., L. Z. and J. L. drafted the manuscript. J. L. and L. Z. proofread and revised the manuscript. All authors reviewed the manuscript, signed this study.

Funding

This work was supported by the National Natural Science Funds (No. 81272833) of China.

Declarations

Ethics approval and consent to participate
Not applicable.

Consent for publication
Not applicable.

Competing interests
The authors declare no competing interests.

ARRIVE guidelines
The manuscript confirming the study is reported in accordance with ARRIVE guidelines.

Additional information
Supplementary Information The online version contains supplementary material available at https://doi.org/10.1038/s41598-025-97887-3.

Correspondence and requests for materials should be addressed to J.L.

Reprints and permissions information is available at www.nature.com/reprints.

Publisher's note Springer Nature remains neutral with regard to jurisdictional claims in published maps and institutional affiliations.